Honokiol Reduces Fungal Load, Toll-Like Receptor-2, and Inflammatory Cytokines in *Aspergillus fumigatus* Keratitis

Lu Zhan,[1] Xudong Peng,[1] Jing Lin,[1] Yingxue Zhang,[2] Han Gao,[1] Yunan Zhu,[1] Yu Huan,[1] and Guiqiu Zhao[1]

[1]Department of Ophthalmology, The Affiliated Hospital of Qingdao University, Qingdao, China
[2]Department of Biochemistry, Microbiology and Immunology, Wayne State University School of Medicine, Detroit, Michigan, United States

Correspondence: Guiqiu Zhao, Department of Ophthalmology, The Affiliated Hospital of Qingdao University, No. 16 Jiangsu Road, Qingdao, 26600 Shandong Province, China;
zhaoguiqiu_good@126.com.

LZ and XP are co-first authors.

Received: December 26, 2019
Accepted: February 24, 2020
Published: April 29, 2020

Citation: Zhan L, Peng X, Lin J, et al. Honokiol reduces fungal load, Toll-like receptor-2, and inflammatory cytokines in *Aspergillus fumigatus* keratitis. *Invest Ophthalmol Vis Sci.* 2020;61(4):48.
https://doi.org/10.1167/iovs.61.4.48

Purpose. We characterized the effects of Honokiol (HNK) on *Aspergillus fumigatus*–caused keratomycosis and the underlying mechanisms. HNK is known to have anti-inflammatory and antifungal properties, but the influence on fungal keratitis (FK) remains unknown.

Methods. In ex vivo, minimum inhibitory concentration and Cell Count Kit-8 assay were carried out spectrophotometrically to provide preferred concentration applied in vivo. Time kill assay pointed that HNK was fungicidal and fungistatic chronologically. Adherence assay, crystal violet staining, and membrane permeability assay tested HNK effects on different fungal stages. In vivo, clinical scores reflected the improvement degree of keratitis outcome. Myeloperoxidase (MPO) assay, flow cytometry (FCM), and immunohistofluorescence staining (IFS) were done to evaluate neutrophil infiltration. Plate count detected HNK fungicidal potentiality. RT-PCR, Western blot, and enzyme-linked immunosorbent assay (ELISA) verified the anti-inflammatory activity of HNK collaboratively.

Results. In vitro, MIC_{90} HNK was 8 µg/mL (no cytotoxicity), and Minimal Fungicidal Concentration (MFC) was 12 µg/mL for *A. fumigatus*. HNK played the fungistatic and fungicidal roles at 6 and 24 hours, respectively, inhibiting adherence at the beginning, diminishing biofilms formation, and increasing membrane permeability all the time. In vivo, HNK improved C57BL/6 mice outcome by reducing disease severity (clinical scores), neutrophil infiltration (MPO, FCM, and IFS), and fungal loading (plate count). RT-PCR, Western blot, and ELISA revealed that HNK downregulated mRNA and protein expression levels of Toll-like receptor-2 (TLR-2), high mobility group box 1 (HMGB1), IL-1β, and TNF-α.

Conclusions. Our study suggested HNK played antifungal and anti-inflammatory roles on keratomycosis by reducing survival of fungi, infiltration of leucocytes, and expression of HMGB1, TLR-2, and proinflammatory cytokines, providing a potential treatment for FK.

Keywords: honokiol, *Aspergillus fumigatus*, keratitis, anti-inflammation, therapeutic potentials

Fungal keratitis (FK) is a serious infectious eye disease in developing countries, associated with agriculture-related ocular trauma, overuse of contact lenses, and post-operative corneal infection, leading to vision loss or blindness.[1,2] *Aspergillus fumigatus* keratitis is one of the most common FK, which tends to result in poor prognosis because of the lack of effective antifungal agents and excessive innate immune response.[3,4] Therefore it is of significance to develop effective antifungal drugs.

Honokiol (HNK; 5,5′-diallyl-2,4′-dihydroxybiphenyl), a natural biphenolic compound extracted from the cortex of *Magnolia officinalis*, is a traditional Chinese herbal material with multiple biological functions, such as anti-tumorigenesis,[5] anti-inflammation,[6,7] antibacterial,[8] and neuroprotective properties.[9] Previous studies suggested that HNK might have an antifungal property.[10]

Fungal infection mainly involves three steps, including adhesion to host cells, hyphal growth, and biofilm formation.[11–16] It has been demonstrated that HNK can inhibit the adhesion and hyphal growth of *Candida albicans* in vitro.[17] Biofilm consists of polysaccharides, polypeptides, and extracellular DNA, which are crucial to protect fungi from being recognized and phagocytosed by the host immune response and increase multidrug-resistant isolates.[18] A previous study showed that HNK could resist the invasion of pathogenic microbials by reducing biofilm formation.[17]

However, the uncontrollable innate immune response is one of the main causes of the poor prognosis of

FK.[19,20] Inflammation-induced recruitment of inflammatory cells, like neutrophils in the cornea, trigger the release of cytokines and chemokines. This release further attracts more immune cells and results in precipitation, causing corneal opacity and vision loss.[19] Thus to control the excessive inflammatory response is the key of FK treatment.[21,22] Interestingly, recent studies showed HNK could attenuate the inflammatory response through inhibiting high mobility group box 1 (HMGB1), Toll-like receptor-2 (TLR-2), and proinflammatory molecules in acute pancreatitis[23] and acute kidney injury[24] in rat models. Here we hypothesized that HNK could provide an alternative to alleviate *A. fumigatus* keratitis through its anti-inflammatory activities.

In this study, we first demonstrated the antifungal and anti-inflammatory roles of HNK in FK mouse models and investigated the underlying mechanisms. Our study may provide a possible therapeutic approach for FK.

Materials and Methods

Preparation of HNK Solution

HNK powder, purchased from MCE (Shanghai, China), was dissolved in PBS (Solarbio, Beijing, China) or other culture mediums at a concentration of 16 µg/mL, and then was diluted with the corresponding mediums as requested.

Cell Viability (CCK-8)

Human corneal epithelial cells (HCECs; provided by Laboratory, University of Xiamen, Fujian, China) (3×10^4/mL) were suspended and seeded in the 96-well plate and treated with HNK (0, 2, 4, 8, and 16 µg/mL) for 12, 24, and 48 hours. The cells were incubated for 2 hours with Cell Counting Kit-8 (CCK-8; MCE), and the absorbance was measured at 450 nm. Each sample had five replicates.

Cell Scratch Test

HCECs (3×10^5/mL) suspension was plated in the 6-well plate and incubated overnight at 37°C. Three parallel lines were scraped on the cell layer using sterile 200 µL pipette tips (Corning, NewYork, USA). The cells were then incubated with HNK (0, 4, 8, and 12 µg/mL) for 24 hours. The width of the scratches observed using an optical microscopy (Axio Vert; Zeiss, Jena, Germany, 100×) were measured before and after HNK treatment.

HNK Minimum Inhibitory Concentration (MIC)

Conidia were harvested by rinsing the *A. fumigatus* (species number 3.0772; General Microbiological Culture Collection Center, Beijing, China) malt agar slants with PBS containing 0.1% Tween 20 (Sigma-Aldrich Corp., St. Louis, MO, USA). Conidia suspension was prepared by repeated resuspending, centrifuging (12,000*g* for 5 minutes), and washing using PBS. MIC HNK for *A. fumigatus* was assayed by a standardized microdilution method in the 96-well plate described as before.[25] Briefly, 100 µL of Sabouraud liquid culture medium was transferred into second to sixth vertical rows. Then removing half of HNK (16 µg/mL, 200 µL) in the seventh column to the left adjacent one realized serial dilutions. Finally, 5 µL of prepared conidia suspension (4×10^6 cfu/mL) was added into the third to seventh columns. The second column was the blank control. The plates were incubated at 37°C without shaking for 36 hours. The HNK MIC_{90} was determined spectrophotometrically, recognized as the lowest concentration that could inhibit 90% growth of *A. fumigatus*.

Time Kill Assay

Based on the MIC, time kill assays were used to evaluate fungicidal/fungistatic activity conveniently and intuitively. As illustrated before,[26] conidia suspension was incubated at 37°C, 120 rpm for 9 hours, and was exposed to HNK (0.5 × MIC, 1.0 × MIC, 1.5 × MIC) for 24 hours. Then the conidial aliquots were plated on the Sabouraud agar plates at different time points (0, 3, 6, 12, 18, and 24 hours), and incubated at 37°C for 18 hours. Fungicidal activity was defined as a reduction in colony count >2log10 cfu/mL, and fungistatic activity was defined as a decrease in colony count <2log10 cfu/mL, compared with cfu on the mediums at the beginning.

Fungal Adherence Assay

Conidia suspension (2×10^5 /mL) containing HNK (0 and 8 µg/mL) was mixed with HCECs and plated on the chambered slides (4/slide) as described previously.[27] Each slide was incubated at 37°C for 3 hours, then washed and stained by hematoxylin and eosin (HE) staining.[28] The spores adhering to HCECs were photographed by an optical microscopy (Axio Vert; Zeiss, Jena, Germany, 400×).

Determination of Biofilm Formation Capacity

The preparation of the microbial inoculum before the biofilm formation was carried out by the standardized microdilution method as described previously.[25] After 48 hours incubation, biofilm was fixed by methanol and then stained with 0.1% crystal violet (Sigma-Aldrich). Rinsing unbound dye repeatedly with PBS, we released the bound dye of the dry biofilm with 95% ethanol. OD was measured at 570 nm three times.

Membrane Permeability

Membrane permeability of HNK was detected using Live/Dead FungaLight Yeast Viability L34952 solutions (Invitrogen, Thermo Fisher Scientific, Waltham, MA, USA) by a flow cytometry (FCM) (CytoFLEX FCM, Beckman Coulter, Indianapolis, IN, USA). Cell samples were stained followed by the experimental protocols to examine cell membrane integrity. All recorded data were analyzed and processed with FlowJo_V10 (Becton, Dickinson, and Company, Franklin Lakes, NJ, USA).

Animal Models of FK

Healthy C57BL/6 mice (female, 8 weeks old) were purchased from Jinan Pengyue Laboratory Animal Co. Ltd. (Jinan, China) and were treated in accordance with the ARVO Statement for the Use of Animals in Ophthalmic and Visual Research. Mice were abdominally anesthetized with 8% chloral hydrate, and intrastromal injections were given using a sterile microliter syringe (10 µL; Hamilton Corp., Bonaduz, GR, Switzerland). After loading 2.5 µL of *A. fumigatus* conidia suspension (2.5×10^7 cfu/mL) into the syringe, it was inserted obliquely into the midstromal level in the center of the right cornea. The left eyes were blank control. Experimental eyes were treated with 5 µL of HNK

Investigative Ophthalmology & Visual Science

Table. Nucleotide Sequence of Mouse Primers Used for RT-PCR

Gene	Nucleotide Sequence	Primer	GenBank
β-actin	5′-GATTACTGCTCTGGCTCCTAG C-3′	F	NM_007393.3
	5′-GACTCATCGTACTCCTGCTTG C-3′	R	
TLR-2	5′-CTCCTGAAGCTGTTGCGTTAC-3′	F	NM_011905.3
	5′-TACTTTACCCAGCTCGCTCACTAC-3′	R	
IL-1β	5′-CGCAGCAGCACATCAACA AGAGC-3′	F	NM_008361.4
	5′-TGTCCTCATCCTGGAAGGTCCACG-3′	R	
TNF-α	5′-ACCCTCACACTCAGATCATCT T-3′	F	NM_013693.3
	5′-GGTTGTCTTTGAGATCCATGC-3′	R	
HMGB1	5′-TGG CAA AGG CTG ACA AGG CTC–3′	F	NM_010439.3
	5′-GGA TGC TCG CCT TTG ATT TTG G-3′	R	

F, forward; R, reverse.

(8 µg/mL) topically, whereas conditional control eyes were treated with PBS topically. HNK topical treatment began at 4 hours post infection (p.i.) and then three times per day (dosing every 4 hours in the daytime) at 1 to 5 days p.i. Subconjunctival injection was given at 16 and 40 hours p.i. Based on the observation under a slit lamp at 1, 3, and 5 days p.i., the severity of keratitis was evaluated by clinical score that was the sum of the three aspects of cornea, including opacity density, opacity area, and surface regularity, each of which has a grade of 0 to 4. Meanwhile, ranging from 0 to 12, the severity of keratitis was divided into normal (0), mild (1–5), moderate (6–9), and severe (10–12). Taking a normal cornea as an example, the unsacrificed cornea was given a score of 0 in each aspect, and thus tallied to yield a score of 0.[29] Mice corneas removed by a scalpel and microscissor at the indicated times after treatments were prepared for RT-PCR, Western blot, myeloperoxidase (MPO), plate count, FCM, and enzyme-linked immunosorbent assay (ELISA), respectively. Then whole eyes were harvested for immunohistofluorescence staining (IFS).

MPO Assay

To determine the activity of polymorphonuclear neutrophils (PMNs) quantitatively,[30] the corneas were harvested at 3 days p.i. (n = 5/group/time) and treated following the protocol of MPO kit (Nanjing Jiancheng Bioengineering Institute, Nanjing, Jiangsu, China). MPO was measured spectrophotometrically at 460 nm at 37°C; the slope of the line was related to the MPO units/g cornea.

Plate Count

The advantage of modified counting was that we could count fungi surviving on the cornea after the treatment. Corneal homogenate after treatment was diluted by PBS, then plated on Sabouraud agar mediums, and incubated at 37°C for 24 hours. Colonies were photographed and counted to reflect fungi surviving on the treated cornea (n = 3/group/time).

FCM Analysis

Neutrophils were shown by monitoring singular cell suspensions stained with fluorescently labeled antibodies. The degree of recruitment was illustrated by the amount and proportion of neutrophils in total inflammatory cells, which were from infected corneas after 3 days treatment. Among the $CD45^+$ cells, $CD11b^+Gr\text{-}1^+$ cells were neutrophils assayed by FCM. The infected corneas of C57BL/6 mice (n = 5/group/time) were treated with PBS or HNK for 3 days t.i.d. topically, harvested and separated into individual cells, and then stained with CD45-PEvio (1:200; Miltenyi Biotec, Bergisch Gladbach, Germany), CD11b-FITC (1:200; BioLegend, San Diego, CA, USA), and Gr-1-PE (1:80; BioLegend) for 20 minutes. FCM was performed according to the manufacturer's instruction, and PMNs were distinguished from leukocytes by staining with CD11b-FITC and Gr-1-PE.

Real-Time RT-PCR

Total RNA of corneas were extracted by the RNAiso plus reagent (TaKaRa, Dalian, China), and the RNA was quantified by a NanoDrop ND-1000 Spectrophotometry (Thermo Fisher Scientific) according to the manufacturer's instructions as described earlier.[30] The extracted mRNA (n = 5/group/time) was used as the template, and cDNA productions (1 µg) were synthesized by a two-step method using PrimeScript RT reagent Kit with gDNA Eraser (TaKaRa). PCR was assayed in 20 µL reaction system (2 µL of diluted cDNA (1:12.5), 10 µL of SYBR Premix Ex TaqTM (TaKaRa), 1 µL of diluted primers (1:9), and 7 µL DEPC-treated water). The PCR program for the reactions was described as before.[31] Analysis of target genes was quantified by the $2^{\Delta\Delta CT}$ method.[32] The corresponding primers are listed in the Table.

Western Blot

The protein separation procedure has been interpreted previously.[33] Six corneas as one sample (n = 6/group/time) were lysed in 196 µL RIPA buffer (Solarbio), 2 µL phenylmethanesulfonyl fluoride (Solarbio), and 2 µL phosphatase inhibitor (MCE) for 2 hours. Protein concentration was determined by BCA assay (Solarbio). Then the proteins were separated by SDS-PAGE electrophoresis and transferred onto polyvinylidene difluoride membrane (Solarbio). After being blocked with blocking buffer (Solarbio), membranes were incubated with primary antibodies against β-actin (1:3000; Elabscience, Wuhan, China), tubulin (1:3000; Elabscience), TLR-2 (1:1000; ABclonal, Wuhan, China), and TNF-α (1:1000; Abcam, Cambridge, MA, USA) at 4°C overnight. The membranes were washed in PBST three times, subsequent to incubation with a secondary antibody at 37°C for 1 hour. Then the blots were visualized using chemiluminescence (Thermo Fisher Scientific).

Immunohistofluorescence Staining

IFS was performed according to the methods described previously.[31] The euthanized mouse eyeballs (n = 3/group/time) were embedded and frozen. A total of

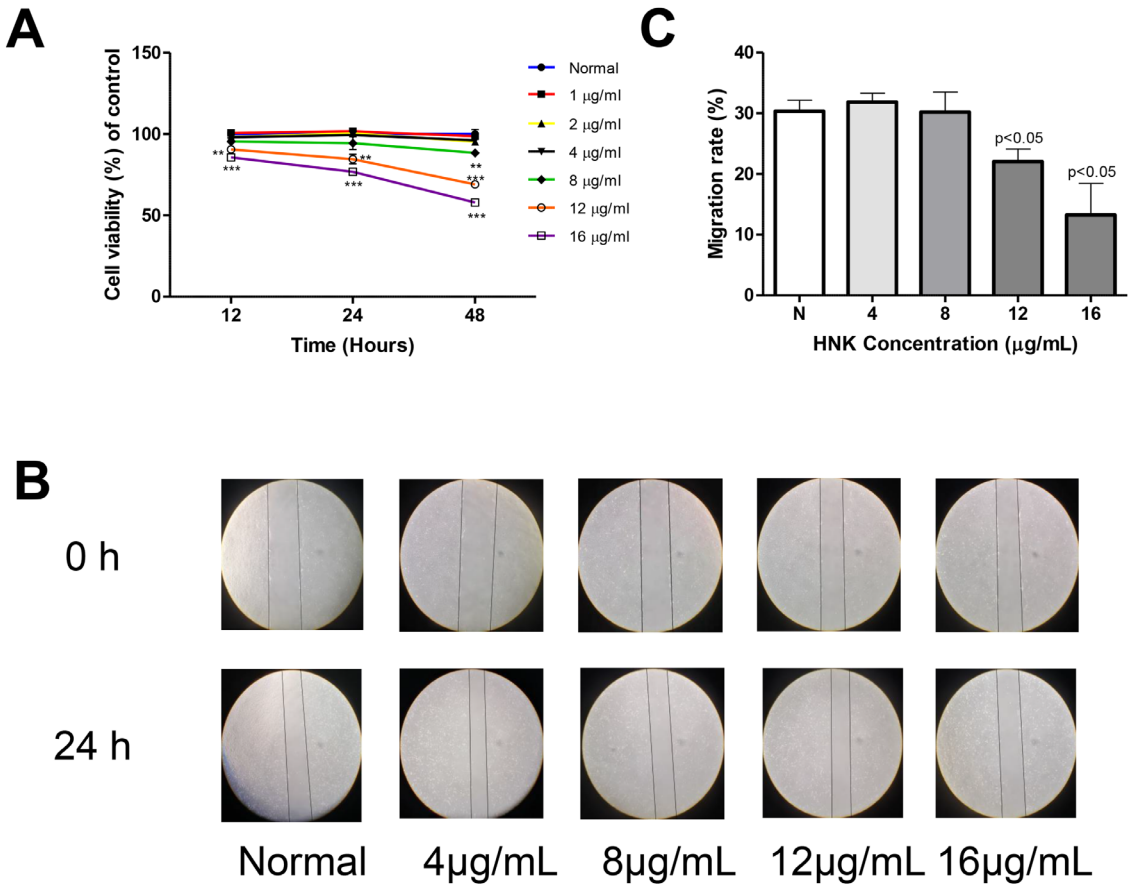

Figure 1. Effects of HNK on cell viability and migration. CCK-8 cell viability assay was performed on HCECs at 12, 24, and 48 hours using different concentrations of HNK (0–16 μg/mL) (**A**). Scratch assay (**B**) and quantitative analysis (**C**) of HNK on re-epithelization potentiality. HNK less than 12 μg/mL hardly affected the migration of HCECs (*P < 0.05, **P < 0.01, ***P < 0.001). All data were mean + SEM and analyzed by an unpaired, two-tailed Student's t-test.

10 μm of corneal lesions were acquired and then fixed in acetone. After being blocked with goat serum (1:100), sections were incubated with monoclonal rat anti-mouse neutrophil marker (1:100; Santa Cruz Biotechnology, Santa Cruz, CA, USA), followed by FITC-conjugated goat anti-rat secondary antibody (1:200; Elabscience). Cell nuclei were stained with DAPI. Images were photographed by a fluorescence microscope (Zeiss Axio Vert, 400×).

Enzyme-Linked Immunosorbent Assay

Following the manufacturer's instructions (Elabscience), individual cornea (n = 5/group/time) was homogenized in 500 μL of PBS containing 1% protease inhibitors (MCE). Undiluted supernatant was quantified using TNF-α, IL-1β, and HMGB1 ELISA kits. The supernatant, diluted two-fold, was used to evaluate the protein level of HMGB1. Sensitivities were as follows: 9.38 pg/mL (HMGB1), 4.69 pg/mL (TNF-α), and 4.69 pg/mL (IL-1β).

Statistical Analyses

Disease score was analyzed by the Mann-Whitney U test (SPSS Statistics 19; IBM Corporation, Armonk, NY, USA), MIC, Cell Scratch Test, RT-PCR, Western blot, and so on by an unpaired, two-tailed Student's t-test (GraphPad Prism; GraphPad, San Diego, CA, USA), and three or more groups by Bonferroni multiple comparison test (GraphPad Prism). These data were median or mean + SEM, P < 0.05 (*P < 0.05, **P < 0.01, ***P < 0.001) as significance. All experiments were performed at least twice to ensure practicability.

Results

HNK Cytotoxicity Test

Cell viability was tested using CCK-8 for different concentrations of HNK in HCECs (Fig. 1A). HNK started to inhibit HCECs proliferation at 8 μg/mL for 48 hours incubation, and no significant cytotoxic effect was observed at 0 to 8 μg/mL for 12 and 24 hours (Fig. 1A). In addition, scratch-wound assay demonstrated that HNK at 8 μg/mL does not affect cell migration compared with control group (Figs. 1B, C). Thus HNK with the concentration no more than 8 μg/mL and incubation time less than 24 hours were considered nontoxic and used in the following in vitro and in vivo experiments.

HNK Inhibits the Growth, Adhesion Ability, and Biofilm Formation of *A. fumigatus*

MIC showed HNK started to inhibit the growth of *A. fumigatus* at 4 μg/mL and prevented 90% *A. fumigatus* growth (MIC_{90}) at 8 μg/mL (Fig. 2A). In the time kill assay, *A. fumigatus* were exposed to HNK at 0.5, 1.0, and 1.5 MIC

Investigative Ophthalmology & Visual Science

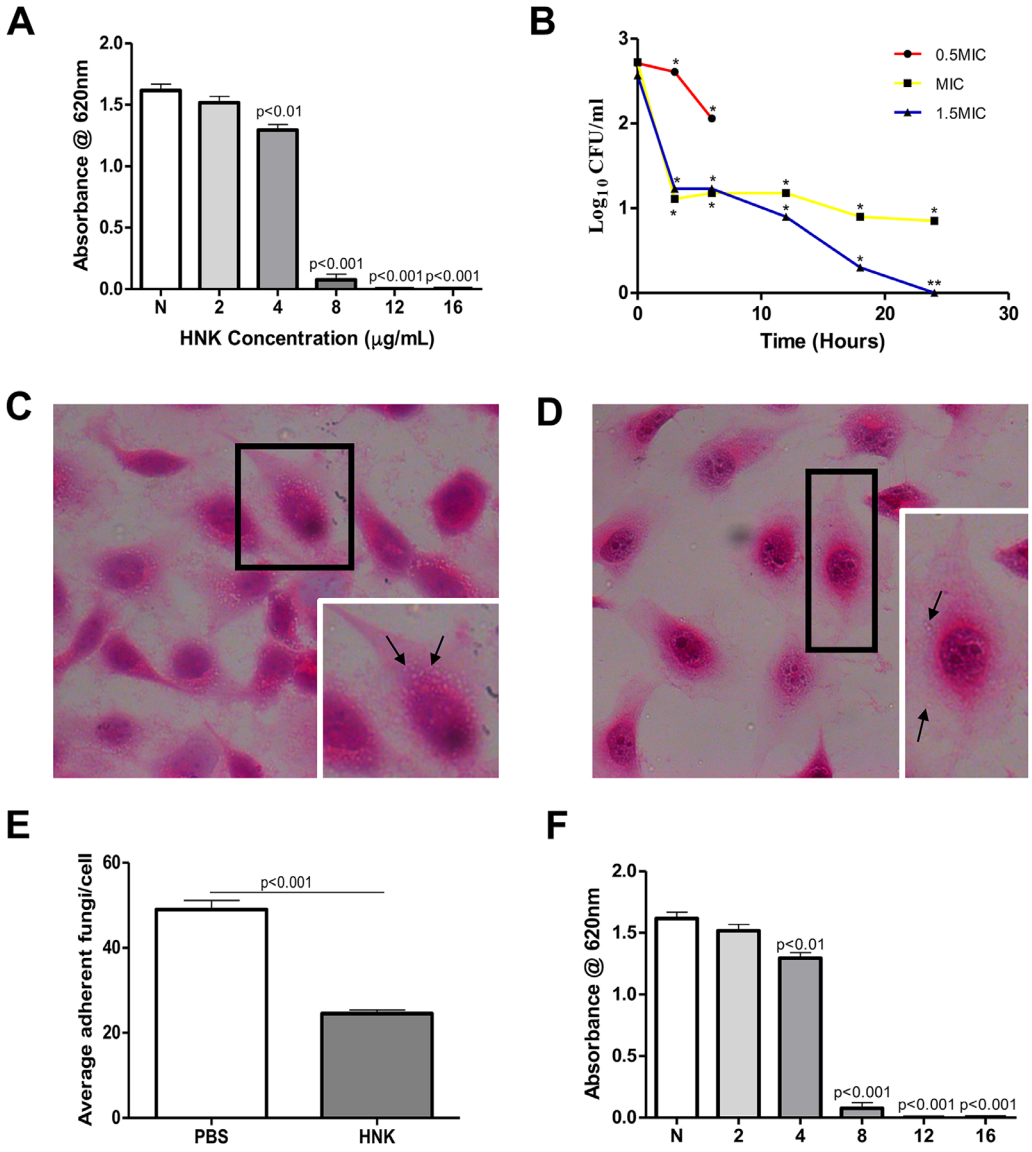

Figure 2. Effects of HNK on MIC, time kill, adherence, biofilm formation in vitro and in vivo. For *A. fumigatus*, MIC_{90} of HNK was 8 μg/mL, MIC_{99} was 12 or 16 μg/mL (**A**). Time kill curves for *A. fumigatus* exposed to 0.5, 1, and 1.5 × MIC of HNK were performed over a period of 24 hours (**B**; *<2log10 cfu/mL, **>2log10 cfu/mL). The *red line* (0.5 × MIC) was incomplete because of the high fungi load. HE staining of *A. fumigatus* infected HCECs treated with PBS (**C**) or HNK (**D**). The cell framed by a *black box* in each panel is magnified in the lower right corner (magnification = ×40 μm). Transparent and rice-like conidia on the cell surface are indicated by *black arrows*, and quantitative diagram is shown at bottom (**E**). Biofilm formation was inhibited significantly by HNK at more than 8 μg/mL in vitro compared with PBS treatment, which was demonstrated by the absorbance values of crystal violet released from the biofilm (**F**). All data were mean + SEM and analyzed by an unpaired, two-tailed Student's *t*-test.

(MIC = 8 μg/mL), which illustrated HNK killed *A. fumigatus* in a time- and concentration-dependent manner. The colony counts were significantly decreased at 1.0 and 1.5 MIC compared with 0.5 MIC, suggesting HNK is effective to kill *A. fumigatus* at 8 μg/mL. Within the first 6 hours, the declined trend of killing fungi was similar between the yellow line (1.0 × MIC) and the blue one (1.5 × MIC). As time went by, the difference between the two lines was obvious. For 0.5 × MIC, we only recorded the formation of colonies within 6 hours. Because fungal colony agglomerated after 6 hours, we failed to count the single units (Fig. 2B). HE staining showed a significant decreased number of adherent conidia on the surface of HNK-treated (8 μg/mL) HCECs compared with PBS-treated cells, indicating HNK inhibits adhesion ability of *A. fumigatus* in HCECs (Figs. 2C–E). Moreover, biofilm formations were tested in HCECs, which suggested HNK at 8 μg/mL remarkably inhibited biofilm formation (Fig. 2F).

HNK Affected Membrane Permeability of *A. fumigatus*

Dead *A. fumigatus* conidia were stained and counted by FCM, showing there were more dead conidia in HNK-treated HCECs (Fig. 3C) than PBS-treated cells (Fig. 3B), which

Investigative Ophthalmology & Visual Science

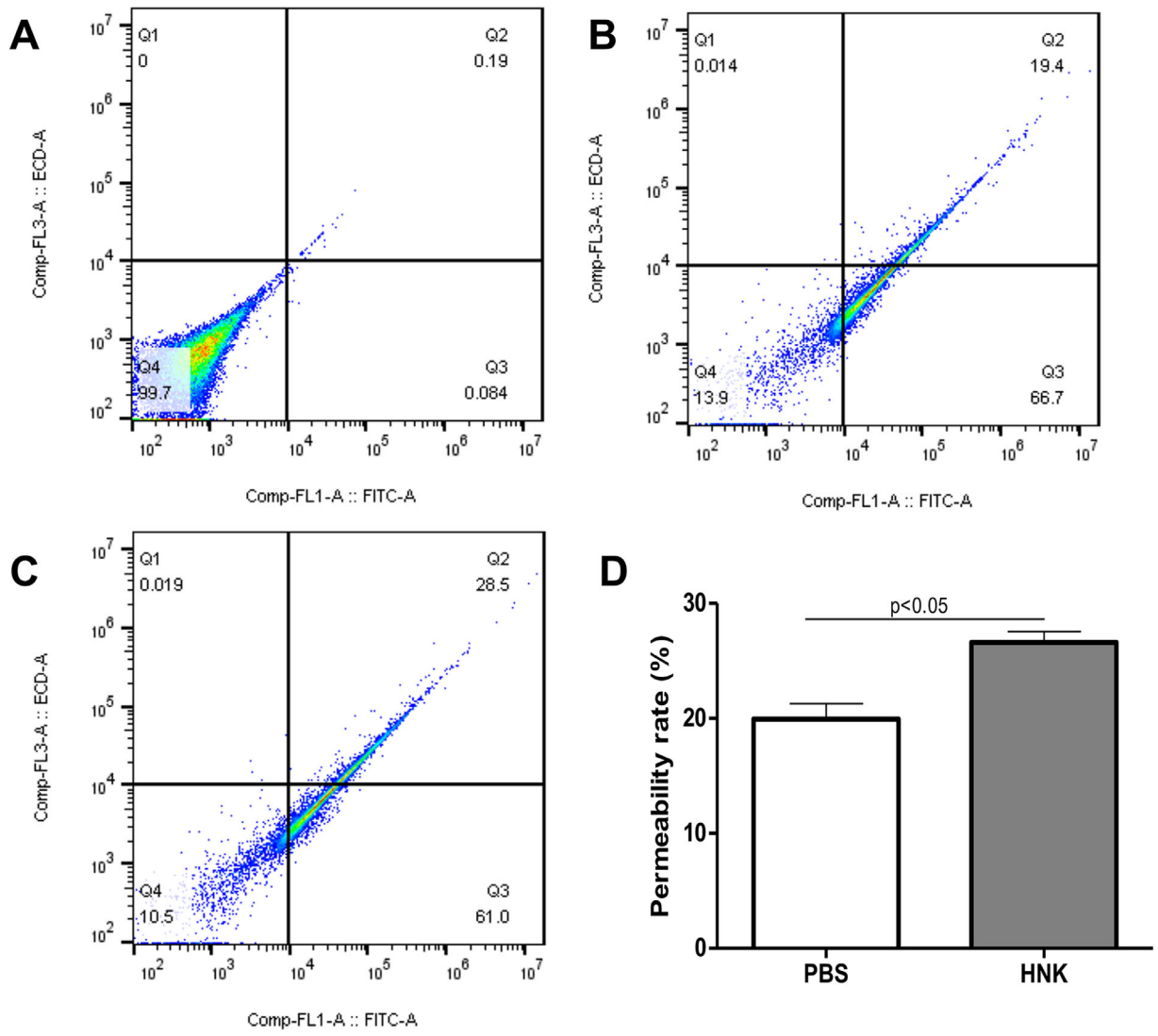

Figure 3. Effect of HNK on membrane permeability. Conidia were tested by a live/dead kit. Unstained live conidia (**A**). The ratio of live and dead cell populations was analyzed and possessed by flow cytometer. Signals of double-stained conidia (FITC-SYTO9 and ECD-PI) are shown in the graphs. Representative PBS treated HCECs (**B**); representative HNK (8 µg/mL) treated HCECs (**C**). The graph shows the difference of ratio of dead conidia between PBS and HNK treatment (**D**; $P < 0.05$). All data were mean + SEM and analyzed by an unpaired, two-tailed Student's *t*-test.

indicates HNK can increase the membrane permeability of *A. fumigatus*. Moreover, a significant increase in the percentage of dead fungi treated with HNK was observed compared with the control (Fig. 3D).

Therapeutic Treatment with HNK

The therapeutic efficacy of HNK was tested with treatment beginning at 1 day p.i. Clinical score in the HNK treatment group was significantly lower than the PBS group at 3 and 5 days p.i., with no difference between groups at 1 day p.i. (Fig. 4A), indicating that HNK could improve corneal transparency and may have corneal protective effects from 3 day p.i. Representative photographs taken with a slit lamp camera illustrated that corneas were more transparent in HNK-treated groups versus PBS control at 1, 3, and 5 days p.i. (Fig. 4B). HNK significantly reduced the neutrophil infiltration at 3 days p.i. (Fig. 4C), and viable fungal load in the infected cornea at 5 days p.i. (Figs. 4D–F).

HNK Reduces the Number and Vitality of Neutrophils in *A. fumigatus* Keratitis Mouse Model

Neutrophils in PBS-treated (Fig. 5A) or HNK-treated (Fig. 5B) mouse cornea were counted using FCM, showing that HNK treatment dramatically reduced the number of neutrophils compared with PBS treatment (Fig. 5D), which is also consistent with immunofluorescence result (Fig. 5E). The neutrophil proportion between the HNK-treated group and control was statistically significant (Fig. 5C). Moreover, MPO results suggested that HNK treatment inhibited neutrophil vitality in *A. fumigatus* keratitis mouse model (Fig. 4C).

Investigative Ophthalmology & Visual Science

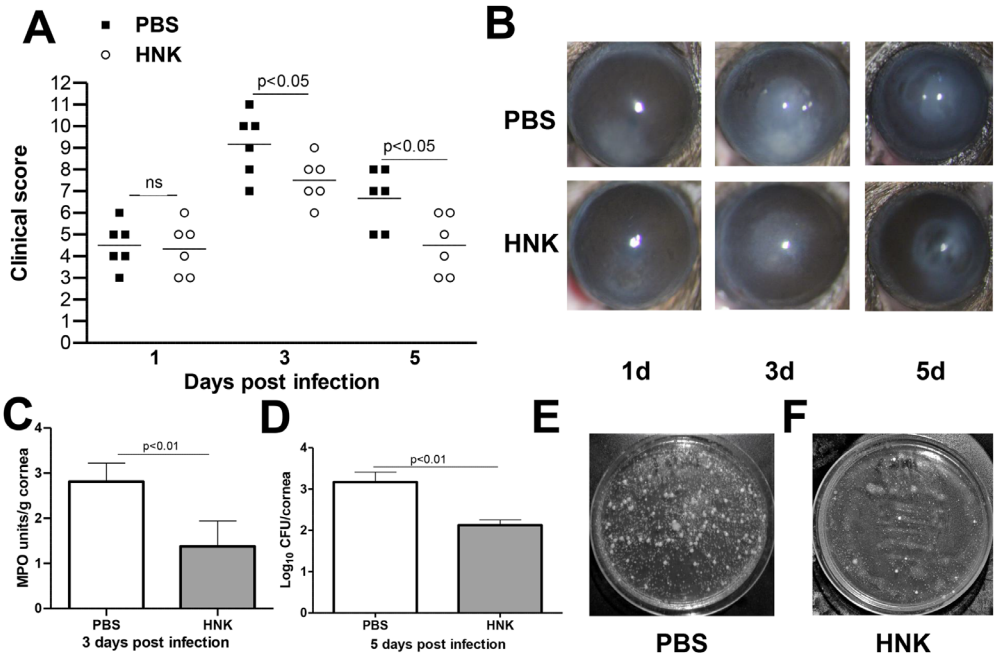

Figure 4. Disease severity after *A. fumigatus* infection followed by PBS or HNK treatment. Clinical sores of PBS or HNK treated *A. fumigatus* keratitis mice at day 1, 3, and 5 (**A**). Representative slit lamp photographs of PBS- or HNK-treated mouse cornea (**B**). Quantitative analysis of MPO at 3 days p.i. (**C**). Representative plates of PBS (**E**) or HNK (**F**) treated *A. fumigatus* infected mouse cornea, and quantitative diagram (**D**). Data were analyzed using a nonparametric Mann-Whitney *U* test. Horizontal lines indicate the median values. Magnification ×8.

HNK Attenuates Inflammatory Response in *A. fumigatus* Keratitis Mouse Model

To detect the effects of HNK in the inflammatory response, we evaluated the mRNA and protein expressions of different inflammatory cytokines at 1, 3, and 5 days after *A. fumigatus* infection. The *A. fumigatus* elevated mRNA expression levels of TLR-2 (Fig. 6A), TNF-α (Fig. 6B), IL-1β (Fig. 6E), and HMGB1 (Fig. 6F), which were significantly repressed by HNK at 3 and 5 days p.i. Similarly, the increased protein expression levels of TLR-2 (Fig. 6C), TNF-α (Fig. 6D), IL-1β (Fig. 6G), and HMGB1 (Fig. 6H) were also inhibited by HNK at 3 and 5 days p.i. For the uninfected corneas (N), no difference in mRNA or protein expression for any cytokines was detected between the HNK and PBS groups.

Discussion

A. fumigatus is one of the most common *Aspergillus* species causing FK in agricultural districts.[34,35] Compared with bacterial ocular infections, presentations of *A. fumigatus* keratitis tend to be more severe because of strong fungal invasiveness and virulence,[36] lack of effective antifungal agents, and long-term use of antibiotic-induced drug resistance. These issues suggest the need to develop more effective antifungal treatments.[35,37,38] HNK is extracted from magnolia bark that is a traditional Chinese herbal material and has been used for thousands of years for its antioxidant, anti-inflammatory, and antibiotic effects.[8,39] Recently, both in vitro and in vivo studies demonstrated that magnolia bark extract has no mutagenic nor genotoxic potential, and no adverse effect was observed for concentrated magnolia bark extract >240 mg/kg body weight/d (mg/kg b.w/d).[40] HNK is one of the main substances of magnolia bark.[41] In this study, we identified that HNK had no cytotoxic effects at 8 µg/mL within 24 hours in HCECs, lending support that HNK could be applied at an appropriate concentration and considered nontoxic. Interestingly, we found that HNK treatment could significantly improve the transparency of mouse cornea with *A. fumigatus* keratitis, relieving the corneal ulcer and protecting cornea integrity. To understand how HNK exhibits the corneal protective effects, we sought to explore its antifungal and anti-inflammatory mechanisms.

We first examined the antifungal effects of HNK. We showed that HNK could inhibit the growth of *A. fumigatus*, which is in agreement with recent studies that HNK inhibited the fungal growth of *Alternaria alternata* and *Fusarium oxysporum*.[42,43] Then we further identified that HNK could repress the adhesion ability and biofilm formation of *A. fumigatus*, which are the critical steps for fungi to infect host cells and resist the host immune system.[44] Furthermore, our data indicated that HNK increased the membrane permeability of *A. fumigatus*, which may cause leakage and imbalance of osmotic pressure between intra- and extracellular membranes, resulting in the irreversible damage to the fungal membrane.[45] Further experimentation could be performed to show which cell membrane component is affected by HNK. In summary, these results demonstrated that HNK has antifungal properties on HCECs through inhibiting the growth, adhesion, biofilm formation, and increasing membrane permeability of *A. fumigatus*, which, to our knowledge, is the first time that these antifungal effects have been confirmed in FK mice and HCECs.

In addition, we tested whether HNK would affect inflammatory response. Innate immune response acts as the first line against fungal infection,[19] however, excessive inflammatory response may contribute to the poor prognosis of FK because of the cornea damage caused by the higher production of proinflammatory factors, cytokines, and oxidative stress.[23,46,47] Neutrophils are professional

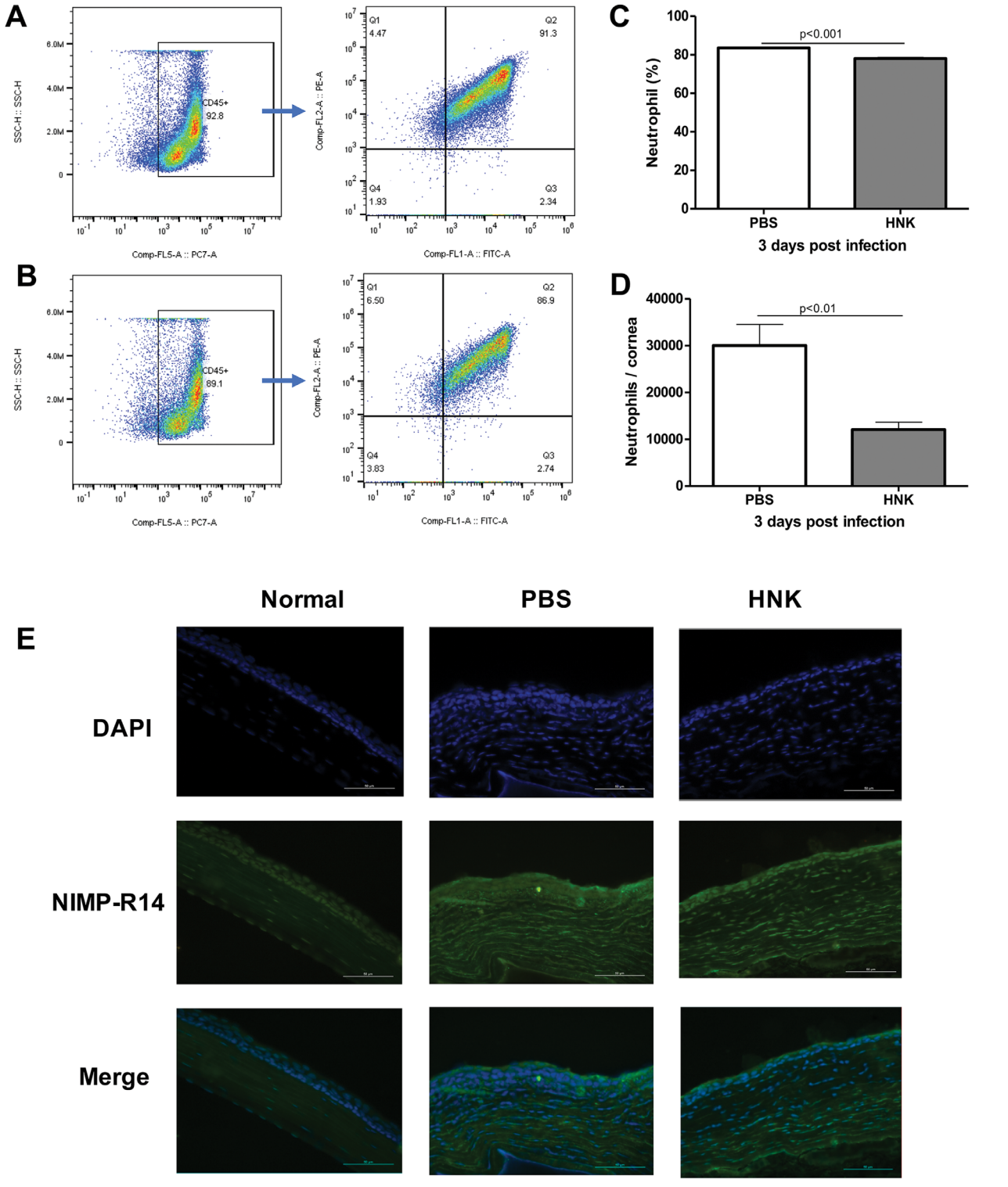

Figure 5. Effects of HNK on neutrophil infiltration. The representative images of recruited and accumulated neutrophils FCM analyzed are shown in **A–D**. Scatter plots gated on CD45+ cells (**A,B**), FCM quantified the mouse cornea infiltrating neutrophils (CD11b+Gr-1+cells) for PBS-treated (**B**) and HNK-treated (**D**) mice at 3 days after *A. fumigatus* infection in the form of representative dot plots, respectively. The outcomes were monitored by the proportion and the number of PMNs (**C,D**). Splenocytes were stained as positive control. (**E**) Immunofluorescent staining demonstrated that HNK treatment reduced neutrophilic infiltrate in the mouse corneal stroma after the fungi infection. NIMP-R14-FITC, neutrophil marker, could specifically label neutrophils. The labeled neutrophils were *green* with a fluorescence microscope. The results showed that the PBS-treated group showed greater staining intensity than the HNK-treated group, which means the larger number of PMN could be observed in the former group. *Green*: NIMP-R14-FITC staining; *blue*: nuclear staining (DAPI) (400×); merge: neutrophil localization. All data were mean + SEM and analyzed by an unpaired, two-tailed Student's *t*-test.

Investigative Ophthalmology & Visual Science

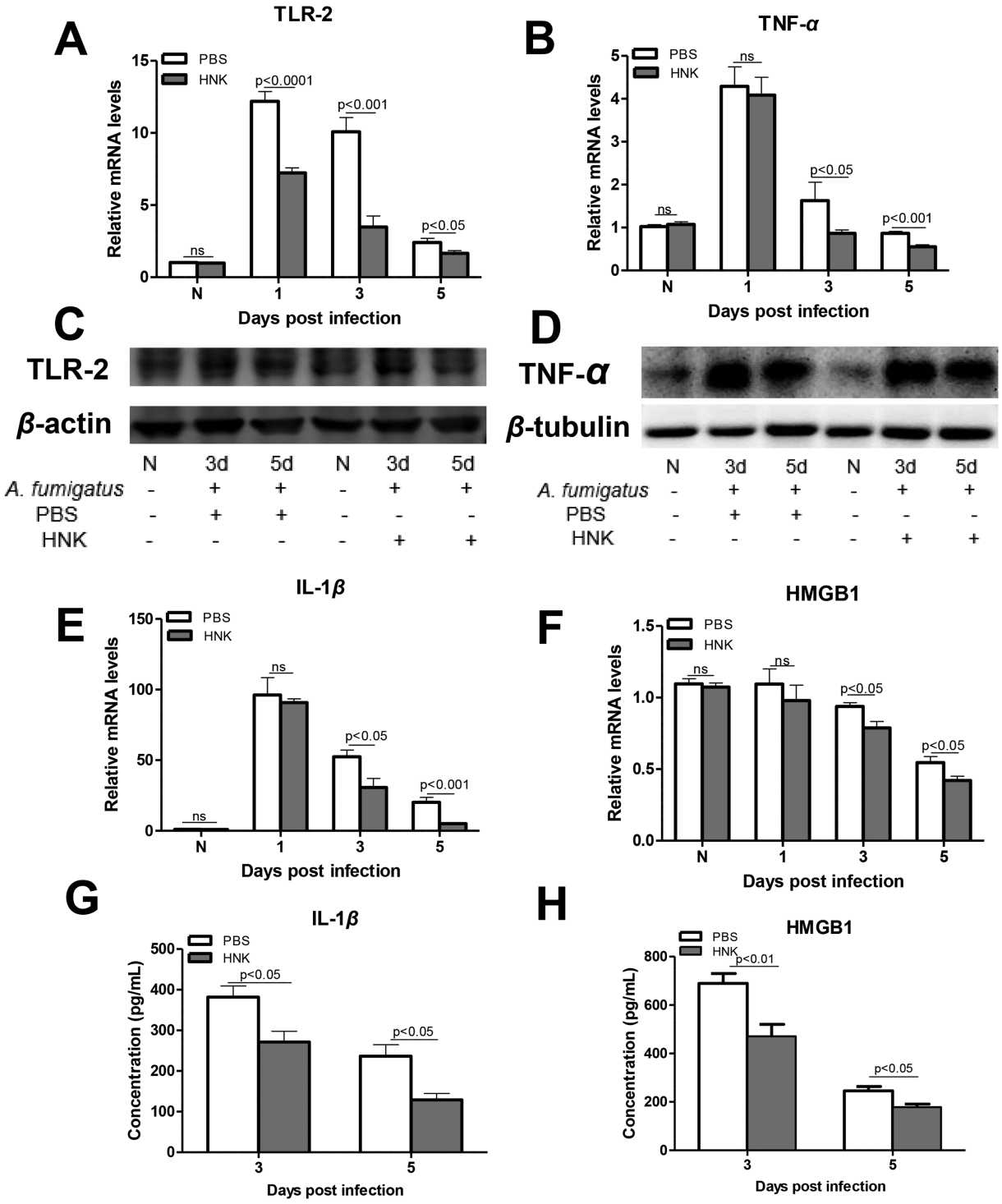

Figure 6. Effects of HNK on the inflammatory response. Real-time PCR results for TLR-2 (**A**), TNF-α (**B**), IL-1β (**E**), and HMGB1 (**F**) at 1, 3, and 5 days after infection in *A. fumigatus* infected mouse cornea and treated with PBS or HNK. In PBS- or HNK-treated *A. fumigatus*–infected mouse cornea, protein expressions of TLR-2, TNF-α, IL-1β, and HMGB1 were detected using Western blot or ELISA. Representative examples of TLR-2 Western blot (**C**) and TNF-α Western blot (**D**) at 3 and 5 days after infection. ELISA results of IL-1β (**G**) and HMGB1 (**H**) at 3 and 5 days after infection. Data were mean + SEM analyzed using an unpaired, two-tailed Student's *t*-test.

phagocytes playing critical roles in fungal infections through various neutrophil pathogen recognition receptors (PRRs), signaling transductions, and cytotoxicity.[48] Still, excessive neutrophil presence can lead to excess monocyte and macrophage recruitment and infiltration, in turn releasing numerous proinflammatory cytokines and chemokines to cause corneal damage.[49] Studies have shown HNK has anti-inflammatory activity,[50,51] and it is reported that HNK not only protects rat brain from focal cerebral ischemia-reperfusion injury through inhibiting neutrophil

infiltration and reactive oxygen species (ROS) production,[52] but also relieves acute pancreatitis via inhibiting expression of TLRs (2/4) and inflammatory mediators, such as TNF-α, IL-1β, and IL-6.[24,53] Thus we investigated whether HNK would influence neutrophil infiltration, as well as the expression of PRRs and proinflammatory mediators in *A. fumigatus* keratitis. Our data suggested that HNK attenuated neutrophil vitality and infiltration to the infected area in vitro and in vivo. Moreover, HNK inhibited the expression of TLR-2 and inflammatory cytokines, including TNF-α, IL-1β, and HMGB1, in *A. fumigatus* HCECs. TLR-2 and TLR-4 activation results in neutrophil activation and the production of ROS, promoting the continuation of the inflammation cycle.[54,55] HNK represses the expression of TLR-2 so that it in turn inhibits neutrophil activation,[56] which is consistent with our result that showed HNK suppressed neutrophil infiltration. This result supports our hypothesis that HNK can inhibit inflammatory response in *A. fumigatus* keratitis. However, the underlying mechanism of the inhibitory effects is still unclear. A few studies suggested HNK could bind to and enhance the activity of deacetylase SIRT3, a class III histone deacetylase predominantly located in mitochondria,[50] and SIRT3 could diminish inflammation and mitigate endotoxin-mediated acute lung injury,[57] which indicates HNK may exhibit its anti-inflammatory effects via mitochondrial function. Further study will be focusing on the exact anti-inflammatory mechanisms of HNK.

Conclusions

Our study demonstrated that HNK has antifungal and anti-inflammatory activities in *A. fumigatus* keratitis mice and HECEs through inhibiting the growth/adhesion/biofilm formation of *A. fumigatus*, increasing fungal membrane permeability, and repressing the expression of TLR-2 and inflammatory cytokines, including TNF-α, IL-1β, and HMGB1. Thus HNK, as a potent antifungal and anti-inflammatory molecule for *A. fumigatus* keratitis, could be a novel therapeutic agent used for FK treatment.

Acknowledgments

Supported by the National Natural Science Foundation of China (No. 81470609; No. 81870632; No. 81500695), and the Natural Science Foundation of Shandong Province (No. ZR2019BH004).

Disclosure: **L. Zhan**, None; **X. Peng**, None; **J. Lin**, None; **Y. Zhang**, None; **H. Gao**, None; **Y. Zhu**, None; **Y. Huan**, None; **G. Zhao**, None

References

1. Peng XD, Zhao GQ, Lin J, et al. Fungus induces the release of IL-8 in human corneal epithelial cells, via Dectin-1-mediated protein kinase C pathways. *Int J Ophthalmol*. 2015;8:441–447.
2. Huang JF, Zhong J, Chen GP, et al. A hydrogel-based hybrid theranostic contact lens for fungal keratitis. *ACS Nano*. 2016;10:6464–6473.
3. Taj-Aldeen SJ. Reduced multidrug susceptibility profile is a common feature of opportunistic fusarium species: fusarium multi-drug resistant pattern. *J Fungi (Basel)*. 2017;3:18.
4. Lalitha P, Prajna NV, Kabra A, Mahadevan K, Srinivasan M. Risk factors for treatment outcome in fungal keratitis. *Ophthalmology*. 2006;113:526–530.
5. Tang H, Zhang Y, Li D, et al. Discovery and synthesis of novel magnolol derivatives with potent anticancer activity in non-small cell lung cancer. *Eur J Med Chem*. 2018;156:190–205.
6. Zhang YM, Zhu L, Zhao XL, et al. Optimal timing for the oral administration of Da-Cheng-Qi decoction based on the pharmacokinetic and pharmacodynamic targeting of the pancreas in rats with acute pancreatitis. *World J Gastroenterol*. 2017;23:7098–7109.
7. Wu H, Yin Z, Wang L, Li F, Qiu Y. Honokiol improved chondrogenesis and suppressed inflammation in human umbilical cord derived mesenchymal stem cells via blocking nuclear factor-kappaB pathway. *BMC Cell Biol*. 2017;18:29.
8. Guo N, Liu Z, Yan Z, et al. Subinhibitory concentrations of honokiol reduce alpha-hemolysin (Hla) secretion by *Staphylococcus aureus* and the Hla-induced inflammatory response by inactivating the NLRP3 inflammasome. *Emerg Microbes Infect*. 2019;8:707–716.
9. Xian YF, Ip SP, Mao QQ, Lin ZX. Neuroprotective effects of honokiol against beta-amyloid-induced neurotoxicity via GSK-3beta and beta-catenin signaling pathway in PC12 cells. *Neurochem Int*. 2016;97:8–14.
10. Lu M, Li T, Wan J, Li X, Yuan L, Sun S. Antifungal effects of phytocompounds on Candida species alone and in combination with fluconazole. *Int J Antimicrob Agents*. 2017;49:125–136.
11. Ferreira AV, Prado CG, Carvalho RR, Dias KS, Dias AL. *Candida albicans* and non-*C. albicans Candida* species: comparison of biofilm production and metabolic activity in biofilms, and putative virulence properties of isolates from hospital environments and infections. *Mycopathologia*. 2013;175:265–272.
12. Ruhnke M. Antifungal stewardship in invasive *Candida* infections. *Clin Microbiol Infect*. 2014;20(Suppl. 6):11–18.
13. Dos Santos Abrantes PM, McArthur CP, Africa CW. Multidrug resistant oral *Candida* species isolated from HIV-positive patients in South Africa and Cameroon. *Diagn Microbiol Infect Dis*. 2014;79:222–227.
14. Haas H. Fungal siderophore metabolism with a focus on *Aspergillus fumigatus*. *Nat Prod Rep*. 2014;31:1266–1276.
15. Ho J, Yang X, Nikou SA, et al. Candidalysin activates innate epithelial immune responses via epidermal growth factor receptor. *Nat Commun*. 2019;10:2297.
16. Kaur S, Singh S. Biofilm formation by *Aspergillus fumigatus*. *Med Mycol*. 2014;52:2–9.
17. Sun L, Liao K, Wang D. Effects of magnolol and honokiol on adhesion, yeast-hyphal transition, and formation of biofilm by *Candida albicans*. *PLoS One*. 2015;10:e0117695.
18. Taylor PK, Yeung AT, Hancock RE. Antibiotic resistance in *Pseudomonas aeruginosa* biofilms: towards the development of novel anti-biofilm therapies. *J Biotechnol*. 2014;191:121–130.
19. Underhill DM, Pearlman E. Immune interactions with pathogenic and commensal fungi: a two-way street. *Immunity*. 2015;43:845–858.
20. Rosowski EE, Raffa N, Knox BP, Golenberg N, Keller NP, Huttenlocher A. Macrophages inhibit *Aspergillus fumigatus* germination and neutrophil-mediated fungal killing. *PLoS Pathog*. 2018;14:e1007229.
21. Brault M, Oberst A. Controlled detonation: evolution of necroptosis in pathogen defense. *Immunol Cell Biol*. 2017;95:131–136.
22. Margalit A, Kavanagh K. The innate immune response to *Aspergillus fumigatus* at the alveolar surface. *FEMS Microbiol Rev*. 2015;39:670–687.
23. Weng TI, Wu HY, Chen BL, Liu SH. Honokiol attenuates the severity of acute pancreatitis and associated lung injury via acceleration of acinar cell apoptosis. *Shock*. 2012;37:478–484.

24. Li N, Xie H, Li L, et al. Effects of honokiol on sepsis-induced acute kidney injury in an experimental model of sepsis in rats. *Inflammation*. 2014;37:1191–1199.
25. Wiederhold NP, Locke JB, Daruwala P, Bartizal K. Rezafungin (CD101) demonstrates potent in vitro activity against *Aspergillus*, including azole-resistant *Aspergillus fumigatus* isolates and cryptic species. *J Antimicrob Chemother*. 2018;73:3063–3067.
26. Balouiri M, Sadiki M, Ibnsouda SK. Methods for in vitro evaluating antimicrobial activity: a review. *J Pharm Anal*. 2016;6:71–79.
27. Cameron OG, Nesse RM. Systemic hormonal and physiological abnormalities in anxiety disorders. *Psychoneuroendocrinology*. 1988;13:287–307.
28. Sun Q, Li C, Lin J, et al. Celastrol ameliorates *Aspergillus fumigatus* keratitis via inhibiting LOX-1. *Int Immunopharmacol*. 2019;70:101–109.
29. Wu TG, Wilhelmus KR, Mitchell BM. Experimental keratomycosis in a mouse model. *Invest Ophthalmol Vis Sci*. 2003;44:210–216.
30. Ekanayaka SA, McClellan SA, Barrett RP, Hazlett LD. Topical glycyrrhizin is therapeutic for *Pseudomonas aeruginosa* keratitis. *J Ocul Pharmacol Ther*. 2018;34:239–249.
31. Yin M, Li C, Peng XD, et al. Expression and role of calcitonin gene-related peptide in mouse *Aspergillus fumigatus* keratitis. *Int J Ophthalmol*. 2019;12:697–704.
32. Peng X, Zhao G, Lin J, Qu J, Zhang Y, Li C. Phospholipase Cgamma2 is critical for Ca(2+) flux and cytokine production in anti-fungal innate immunity of human corneal epithelial cells. *BMC Ophthalmol*. 2018;18:170.
33. Peng X, Zhao G, Lin J, Li C. Interaction of mannose binding lectin and other pattern recognition receptors in human corneal epithelial cells during *Aspergillus fumigatus* infection. *Int Immunopharmacol*. 2018;63:161–169.
34. Yang X, Zhao G, Yan J, et al. Pannexin 1 channels contribute to IL-1beta expression via NLRP3/caspase-1 inflammasome in *Aspergillus fumigatus* keratitis. *Curr Eye Res*. 2019;44:716–725.
35. Kredics L, Narendran V, Shobana CS, Vagvolgyi C, Manikandan P; Indo-Hungarian Fungal Keratitis Working Group. Filamentous fungal infections of the cornea: a global overview of epidemiology and drug sensitivity. *Mycoses*. 2015;58:243–260.
36. Thomas PA, Kaliamurthy J. Mycotic keratitis: epidemiology, diagnosis and management. *Clin Microbiol Infect*. 2013;19:210–220.
37. Cole DC, Govender NP, Chakrabarti A, Sacarlal J, Denning DW. Improvement of fungal disease identification and management: combined health systems and public health approaches. *Lancet Infect Dis*. 2017;17:e412–e419.
38. Falcone EL, Holland SM. Invasive fungal infection in chronic granulomatous disease: insights into pathogenesis and management. *Curr Opin Infect Dis*. 2012;25:658–669.
39. Ochoa C, Solinski AE, Nowlan M, Dekarske MM, Wuest WM, Kozlowski MC. A bisphenolic honokiol analog outcompetes oral antimicrobial agent cetylpyridinium chloride via a membrane-associated mechanism. *ACS Infect Dis*. 2020;6:74–79.
40. Sarrica A, Kirika N, Romeo M, Salmona M, Diomede L. Safety and toxicology of magnolol and honokiol. *Planta Med*. 2018;84:1151–1164.
41. Lee YJ, Lee YM, Lee CK, Jung JK, Han SB, Hong JT. Therapeutic applications of compounds in the Magnolia family. *Pharmacol Ther*. 2011;130:157–176.
42. Chen YH, Lu MH, Guo DS, et al. Antifungal effect of magnolol and honokiol from *Magnolia officinalis* on *Alternaria alternata* causing tobacco brown spot. *Molecules*. 2019;24:2140.
43. Oufensou S, Scherm B, Pani G, et al. Honokiol, magnolol and its monoacetyl derivative show strong anti-fungal effect on *Fusarium* isolates of clinical relevance. *PLos One*. 2019;14:e0221249.
44. Beauvais A, Latge JP. *Aspergillus* biofilm in vitro and in vivo. *Microbiol Spectr*. 2015:3.
45. Yan T, Han J, Yu X. E-cadherin mediates adhesion of *Aspergillus fumigatus* to non-small cell lung cancer cells. *Tumour Biol*. 2016;37:15593–15599.
46. Cuesta V, Singhal R, de la Cruz P, Sharma GD, Langa F. Near-IR absorbing D-A-D Zn-porphyrin-based small-molecule donors for organic solar cells with low-voltage loss. *ACS Appl Mater Interfaces*. 2019;11:7216–7225.
47. Yu Y, Li M, Su N, et al. Honokiol protects against renal ischemia/reperfusion injury via the suppression of oxidative stress, iNOS, inflammation and STAT3 in rats. *Mol Med Rep*. 2016;13:1353–1360.
48. Gallagher D, Siddiqui F, Fish J, et al. Mesenchymal stromal cells modulate peripheral stress-induced innate immune activation indirectly limiting the emergence of neuroinflammation-driven depressive and anxiety-like behaviors. *Biol Psychiatry*. 2019;86:712–724.
49. Moretti S, Bozza S, Massi-Benedetti C, et al. An immunomodulatory activity of micafungin in preclinical aspergillosis. *J Antimicrob Chemother*. 2014;69:1065–1074.
50. Pillai VB, Samant S, Sundaresan NR, et al. Honokiol blocks and reverses cardiac hypertrophy in mice by activating mitochondrial Sirt3. *Nat Commun*. 2015;6:6656.
51. Cho JH, Jeon YJ, Park SM, et al. Multifunctional effects of honokiol as an anti-inflammatory and anti-cancer drug in human oral squamous cancer cells and xenograft. *Biomaterials*. 2015;53:274–284.
52. Liou KT, Shen YC, Chen CF, Tsao CM, Tsai SK. Honokiol protects rat brain from focal cerebral ischemia-reperfusion injury by inhibiting neutrophil infiltration and reactive oxygen species production. *Brain Res*. 2003;992:159–166.
53. Xiang H, Zhang Q, Qi B, et al. Chinese herbal medicines attenuate acute pancreatitis: pharmacological activities and mechanisms. *Front Pharmacol*. 2017;8:216.
54. Lentini G, Fama A, Biondo C, et al. Neutrophils enhance their own influx to sites of bacterial infection via endosomal TLR-dependent Cxcl2 production. *J Immunol*. 2019:ji1901039.
55. Asanka Sanjeewa KK, Jayawardena TU, Kim HS, et al. Fucoidan isolated from *Padina commersonii* inhibit LPS-induced inflammation in macrophages blocking TLR/NF-kappaB signal pathway. *Carbohydr Polym*. 2019;224:115195.
56. Xia S, Lin H, Liu H, et al. Honokiol attenuates sepsis-associated acute kidney injury via the inhibition of oxidative stress and inflammation. *Inflammation*. 2019;42:826–834.
57. Kurundkar D, Kurundkar AR, Bone NB, et al. SIRT3 diminishes inflammation and mitigates endotoxin-induced acute lung injury. *JCI Insight*. 2019;4:e120722.

Investigative Ophthalmology & Visual Science